

International Conference on Space Optics—ICSO 2018

Chania, Greece

9–12 October 2018

Edited by Zoran Sodnik, Nikos Karafolas, and Bruno Cugny



Validation of a spatial light modulator for space applications

Manuel Silva-López

Antonio Campos-Jara

Alberto Álvarez-Herrero



International Conference on Space Optics — ICSO 2018, edited by Zoran Sodnik,
Nikos Karafolas, Bruno Cugny, Proc. of SPIE Vol. 11180, 111806R · © 2018 ESA
and CNES · CCC code: 0277-786X/18/\$18 · doi: 10.1117/12.2536162

Validation of a spatial light modulator for space applications

Manuel Silva-López*, Antonio Campos-Jara, Alberto Álvarez Herrero
Instituto Nacional de Técnica Aeroespacial (INTA), Área de Instrumentación Óptica Espacial,
carretera de Ajalvir, Km. 4, Torrejón de Ardóz, 28850 Madrid, Spain

ABSTRACT

Liquid crystals on silicon spatial light modulator (LCOS-SLM) combine the potential of reflection type spatial light modulators with the compactness and robustness of a single chip. They are used today for beam steering applications, optical beam shaping and laser processing. These devices have a high potential for space applications due to the fact that they allow to introduce any tailored wavefront distortion in an imaging instrument. Then, image reconstruction methods as phase diversity can be used to determine the Point Spread Function (PSF) inflight and, later, to introduce a corrective wavefront distortion to correct possible deviations of the expected optical quality.

Among other aberrations, the beam phase control can act on the level of focus. In space optical applications image refocusing is usually performed by means of mechanisms, either by using linear displacement of lenses or rotating wheels with plates with different thicknesses. The compactness and absence of mechanical parts of LCOS-SLM can be of great advantage for these applications. LCOS-SLM can save complexity and weight. It also reduces the risk associated to the wear of moving parts.

However, this technology has not been qualified for space applications. Liquid crystal leaks as well as outgassing issues may result as a consequence of a low pressure environment. Thermal issues can also result in loss of device homogeneity and the radiation tolerance should be analyzed. In any case, an exhaustive space simulation test is mandatory to increase the Technological Readiness Level of these devices for their use in space systems.

In our work we are showing preliminary test of a commercial LCOS-SLM under thermo-vacuum conditions. These tests are basic calibrations used to evaluate performance and degradation in a simulated space environment. Different calibration procedures are also discussed. This technology, with potential to greatly simplify an instrument design, was included in a proposal for the instrument IMaX+ spectro-polarimeter, to be onboard the mission Sunrise III, within the NASA Long Duration Balloon program.

Keywords: Spatial light modulator, liquid crystal, polarimetry, phase shifting, space application

1. INTRODUCTION

A LCOS-SLM is an electrically addressed, reflection type, phase 2D spatial light modulator. Liquid crystals on silicon yields a structure where a liquid crystal layer, serving as the light modulating part, is arranged on an electrically addressing part formed by CMOS technology. I.e. liquid crystal is controlled by a direct voltage, and can modulate the wavefront of a light beam. They have found applications in optical beam shaping, aberration correction, optical manipulation and laser material processing [1], [2].

In space applications, were resources such as mass, volume, power consumption and reliability are fundamental issues; there is a strong demand on photonic devices. Liquid crystal devices, in particular, can be developed and implemented to avoid mechanical parts on spacecraft optical instrumentation. Indeed, some preliminary tests have been published evaluating the space survivability of this technology [3]. Following this aim we performed an extensive validation campaign of liquid crystals for aerospace applications [4]. Because of this work, polarization modulators based on liquid crystal variable retarders are used in remote sensing instruments on board the Solar Orbiter mission, from the European Space Agency [5]. Alternatively, in communication systems, this technology allows developing of non-mechanical laser beam steering technology, which provides advantages for stablishing satellite-to-ground data links [6].

The beam phase control that a LCOS-SLM provide may compensate aberrations in on board imaging instruments. Phase diversity technics and defocus correction can be easily implemented. This alternative arrangement can reduce weight and

*silvalm@inta.es

complexity since no mechanical devices (such as rotating wheels or refocusing mechanisms are required). An LCOS can also encode information in the beam reflected wavefront allowing free-space quantum communication.

Still some issues may limit its final application. The time response is typically of milliseconds (for nematic type liquid crystals), and quantum key distribution demand for a GHz bandwidth. The sensitivity to the space environment, this is: vacuum, particle, ionizing and non-ionizing radiation tolerance and the thermal environment require a careful system design and qualification process.

As a consequence, due to the substantial interest in utilizing these devices in space, we have performed numerous tests to explore the potential suitability of the LCOS technology for space applications. The final aim of this preliminary work is to push the technological readiness level (TRL), to a TRL 5. This level is defined by a critical function verification in a relevant environment. This milestone is achieved when performance is verified through testing in the relevant environment, subject to scaling effects [7].

Thus, in our work we have chosen a commercial LCOS-SLM and choose a number of figures of merit to be evaluated before, during and after setting the device in the vacuum conditions. Although there are different calibration methods [8], [9], we have chosen the following methods: The first is the modulation transfer characteristic, a measure of the change of phase relative to zero grey value displayed on the SLM. This is equivalent to the characteristic retardance versus voltage curve, typical for a liquid crystal cell. Then the response time is evaluated using the transmitted light method. Finally the LCOS surface flatness is also evaluated using a phase shifting technique. The last is relevant since the change of pressure may cause the liquid crystal cavity spacing to change.

2. LIQUID CRYSTAL ON A CHIP

In our work we have used a LCOS-SLM (Model X10468-01) from Hamamatsu. This comes in a compact head of 74×39×110 mm external dimensions. The LCOS active area is formed of a glass substrate, a transparent electrode, alignment film, and a parallel-aligned nematic liquid crystal layer on top of an aluminum mirror and a silicon substrate. An active matrix circuit is formed on the silicon substrate for applying voltages to pixel electrodes. Thus the amount of phase modulation varies according to the applied voltage level.

The LCOS main characteristics are listed in Table 1. It can achieve phase modulation of more than 2π radians over the visible wavelength range. The voltage applied to each pixel in the device is assigned through a look up table programmed in the LCOS control software. Basically the LCOS display works as an extended monitor. Eight-bit grey images are displayed according to the voltages applied on each pixel.

The LCOS head is connected by means of two cables to the LCOS controller. The controller processes the images sent from the PC via the DVI-D cable and sends the suitable control signals to the LCOS.

Table 1. LCOS characteristics

Parameter	Specification	Parameter	Specification
Number of pixels	792 × 600	Phase resolution	0.009 π / level
Pixel pitch (μm)	20	Rise time (ms)	5
Effective area size (mm)	16 × 12	Fall time (ms)	25
Fill factor (%)	98	Light utilization efficiency (%)	79
Input signal levels	256 for 8bit	Operating temperature ($^{\circ}\text{C}$)	10 to 40
Wavelength range	400 to 700 nm	Storage temperature ($^{\circ}\text{C}$)	-20 to 55
Maximum phase modulation (rad)	2.28 π	Operating pressure (altitude in m)	<2000

3. EXPERIMENTAL SET UP

The experimental setup is shown in Figure 1. A He-Ne laser beam is expanded and collimated to cover the whole LCOS effective area. A beam splitter folds the LCOS reflected light path so that a detector or a camera, depending on the type of measurement to be performed, is illuminated. A reference mirror, also shown in Figure 1, is only used when the interferometer arrangement is set up.

To simulate the space environment a thermal vacuum chamber (TVC) was used. The TVC has a cylinder shape with 26 cm of inner diameter and 28 cm height. It provides feedthroughs for connections to thermo-electric elements and the LCOS head. In order to prevent any overheating, two thermocouples were attached to the front and back part of the modulator. The TVC has an optical window that allows the LCOS illumination and a dedicated feedthrough was built to interface the LCOS head with the controller. Finally, a primary pump and a turbomolecular pump (Varian, Turbo-V 81-M) connected to the TVC sets the vacuum levels required for the tests.

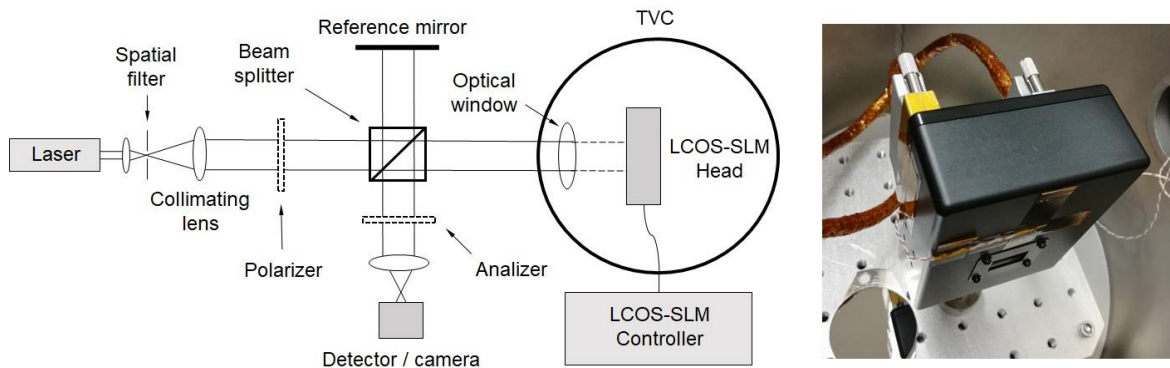


Figure 1. Set up configuration employed to obtain the phase modulation characteristic (with reference mirror blocked and using a detector). This setup is then adapted to perform surface flatness measurements (using the camera a no polarizers). Picture at the right side shows a view of the LCOS head inside the TVC.

Using this arrangement four sets of measurements were performed. First, a study of the LCOS performance was carried out at room conditions, and the parameters compared to the ones specified by the manufacturer. Then the LCOS was subject to vacuum conditions (~ 1 mbar) during 24 hours. Following this, we study again performance at room conditions. The aim of this stage is to evaluate device degradation in vacuum at non-operative conditions. The third set of measurements is carried out during an operative test at vacuum conditions. Finally, a post vacuum operative test at room conditions will set the final performance.

4. MEASUREMENT METHODS

4.1 Transfer characteristic

To obtain the transfer characteristic the reference mirror shown in Figure 1 is actually blocked and the reflected beam from the LCOS is focused on a photodetector (model 818 UV, Newport). Since the LCOS liquid crystal molecules are horizontally aligned (0°), the polarization direction of the incident light is adjusted (by means of a polarizer) to 45° . Upon reflection on the LCOS active area, the light beam travels through an analyzer, which is set to 90° with respect to the polarizer. Thus, this setup measures intensity changes as flat images of gray levels (256 provided by 8-bit pixel values) are displayed in the LCOS. The phase value (ϕ) can be determined from the measured light intensity by means of

$$I = I_o \sin^2(\phi/2) \quad (1)$$

A preliminary measurement provides a linear response with a phase resolution of 0.00948π / level with a maximum phase modulation of 2.41π rad.

4.2 Response time

Using the experimental arrangement described in the previous section the response time can also be measured. By sending a sequence of grey images corresponding to 0 and 2π we can obtain the response time characteristics with the detector connected to an oscilloscope. When the LCOS is switched between these two states the measured change in the output light level is converted into a phase change and the rise/fall times required for a transition is calculated. We have used A Foton Focus photodetector selecting the 10k- Ω resistor mode with 50 ns typical response speed according to the manufacturer.

Thus, the response time can be evaluated by means of the transmitted light measurement method [10]. Since the phase shift is higher than π rad, it is expected that the time-dependent intensity signal $I(t)$ captured will contain overshoot and undershoot phenomena. In order to simplify the analysis a $\phi(t)$ inversion has been done using Equation 1, [11]. Consequently, we can calculate the rise and fall time directly from the phase over time curves as the time elapsed between 10% and 90% of the total phase shift signal. The values presented in this work are the mean of twenty measurements for each type of transition.

Figure 2 shows examples of the signals obtained and the rise/fall time calculated. These measurements were obtained at room conditions and before the vacuum tests. They are slightly faster than the manufactures specification.

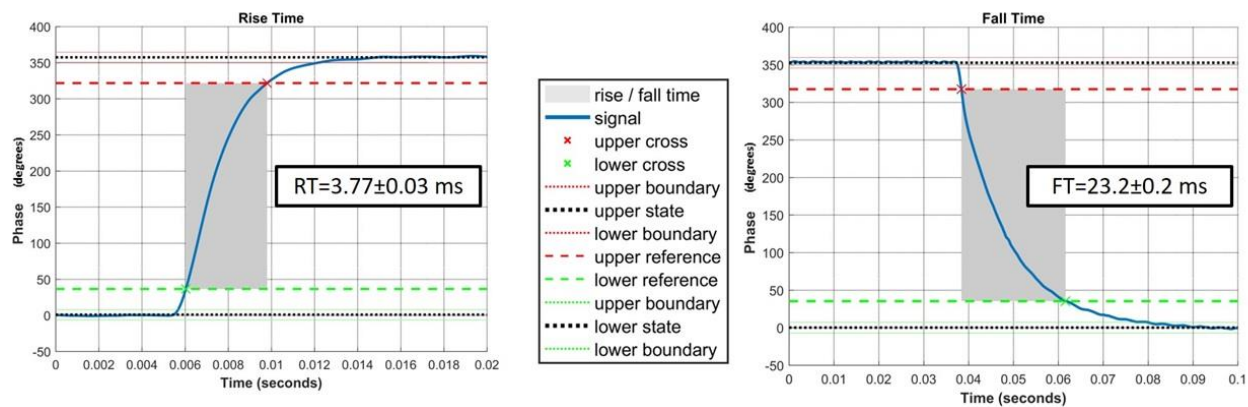


Figure 2. Rise and fall time as measured from a 2π phase jump/transition at room conditions before the vacuum tests

4.3 Surface flatness

As it was mentioned, the liquid crystal cavity may change with pressure. Moreover, due to fabrication limitations, the silicon back plane and glass substrate of the SLM may not be flat nor parallel. This contributes to the nonlinearity of the response, since the induced phase delay is proportional to thickness. Thus, an inspection of the surface flatness of the device is mandatory during the tests, and has been performed by fringe pattern analysis.

Interferometer patterns are captured by a camera using the setup shown in Figure 1. The reference mirror is unblocked and the polarizers are removed. Spatial light modulators allow using a special type of phase shifting method: The reference mirror is set static and different wavefronts are excited by means of the modulator. A four-square mask, shown in Figure 3a), is sent to the LCOS. The squares are set 44 levels of grey apart (0.42π rad). From image to image, a constant offset is added to this mask, thus simulating a moving reference mirror.

We have chosen the 5-step Hariharan method [12], as a good compromise between measurement time and accuracy. Therefore five fringe patterns, as the one illustrated in Figure 3b), are captured by the camera. Then a low pass filter is applied to each fringe image in order to remove high frequency noise.

For the 2D phase unwrapping process we used the Itoh algorithm [13]. This is a simple algorithm suitable when images have low noise and do not contain phase jumps. With this we obtain an unwrapped phase surface which spans many radians (depending on the number of fringes in the images). This is due to a tilt contribution that can be removed by fitting a plane to the data. An example of the final unwrapped phase image with tilt removed can be seen in Figure 3c)

and d). The original four-square pattern sent to the modulator can be seen. Although quite similar, the phase image has clear differences from the original pattern, especially at the edges. This recovered pattern can be used to further calibrate the modulator. We have evaluated the wavefront shape recovered by the phase shifting method and the rms.

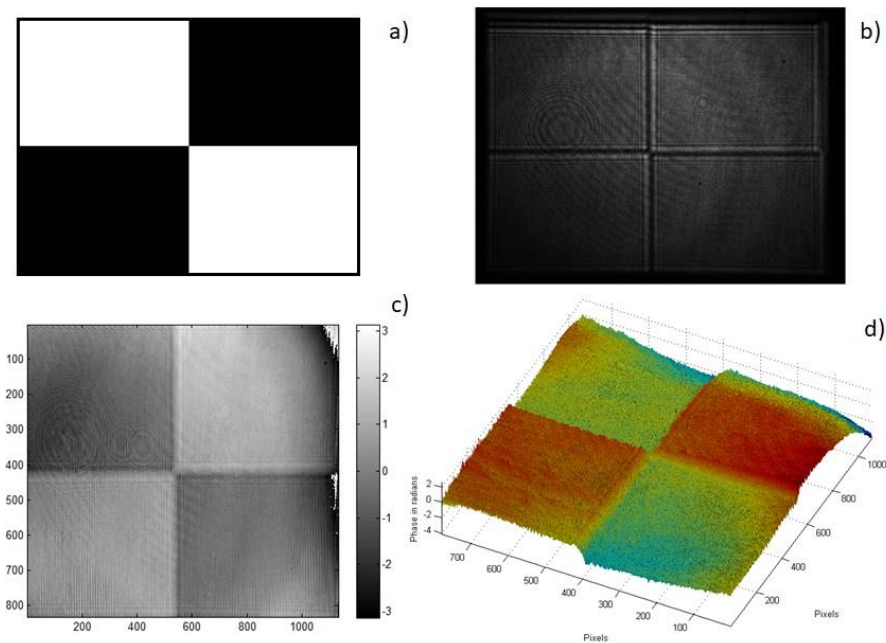


Figure 3. Measurement and processing. a) image sent to modulator, b) fringe pattern obtained in the interferometer and c) and d) unwrapped phase image with tilt removed

4.4 Thermal issues

As a commercial multi purpose device, the LCOS has not been designed to withstand extreme temperatures, as seen in Table 1. At vacuum conditions the device will tend to heat up since no air will be available to cool the device down. Thus, to evaluate heat dissipation a number of infrared images were obtained at room conditions from the LCOS head using an infrared camera (Thermo Vision A320, FLIR Systems). This provides a first approximation to the thermal gradient present in a working device. The thermal images showing the LCOS front side are illustrated in Figure 4. After a few minutes ON it can be observed that the active area is heated up nearly 1°C. This may be due to the warming up of the CMOS chip at the backplane. Moreover, liquid crystal birefringence decreases as the temperature increases. Thermal control is assumed, many liquid crystal based devices use temperature stabilization routines to maintain calibration temperature. Around the effective area no other hot spots were revealed.

In any case, a pair of thermocouples were attached to the LCOS head so that thermal monitoring could be performed during the vacuum tests to prevent any overheating.

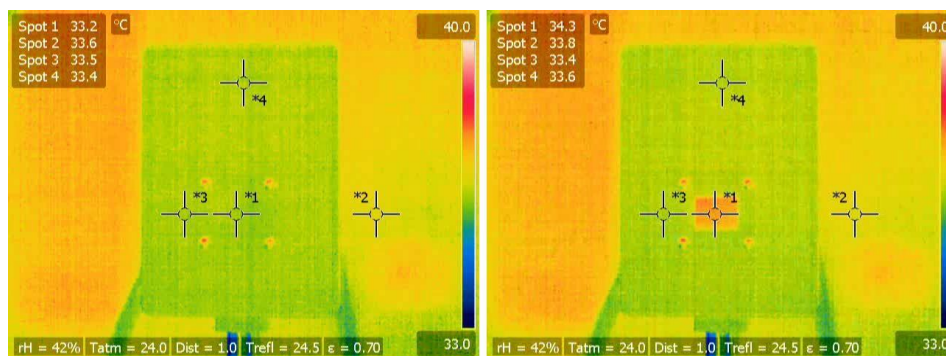


Figure 4. Thermal images obtained using an infrared camera. Left: Image of the LCOS front side OFF. Right: After a few minutes ON.

4.5 Efficiency

This LCOS model is an aluminum mirror type which provides a wider wavelength range. However, dielectric mirror types deliver more than 90% light utilization efficiency, and aluminum mirror types offer 70 to 83%. Loss of light level is mainly caused by generation of diffracted light resulting from the pixel structure, scattering in the liquid crystal layer, and absorption by the transparent electrode [2].

On the other hand the diffraction efficiency is governed by the inter-pixel distance (or fill factor). Indeed pixelated SLMs diffract light into higher orders, which reduces device efficiency and causes sidelobe interference. The ideal is a smooth pixel to pixel phase transition that allows the device to operate as a continuous deformable mirror. Recent advancements have increase the fill factor to nearly 100% [14].

5. RESULTS

In this section, we summarized the figures of merit described earlier as we have proceed with the tests. Figure 5 shows the phase modulation transfer at each point during the campaign. The difference between the curves can be explained by different experimental conditions. This is due to different detector and polarizer's position every time the experimental arrangement was set. This may be improved in the future with a dedicated setup. The data scattering around a linear fit is within $\pm 5^\circ$ ($\pm 0.027\pi$ rad).

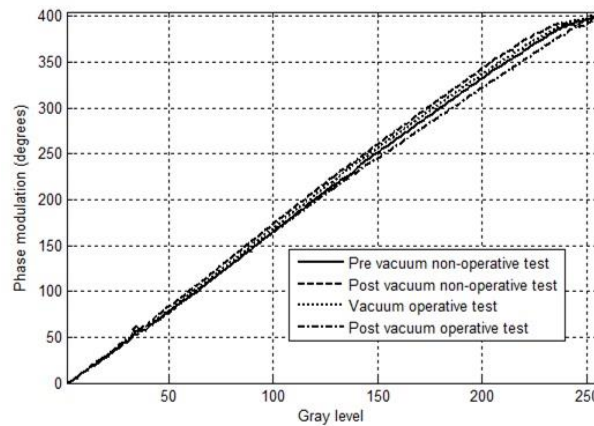


Figure 5. Phase change as a function of the grey value displayed in the spatial light modulator. Different curves correspond to different stages of the test campaign.

Table 2 summarizes the main parameters evaluated experimentally. The first row corresponds to the ratio between the phase change and the grey level displayed in the modulator, as it was shown in Figure 5. The second and third row illustrates the rise and fall time obtained at each stage. The different span in the uncertainty obtained may be due to repeatability issues associated to the experimental arrangement, which is set up and aligned each time the test conditions are changed. Finally the rms of the wavefronts recovered are listed in the last row of Table 2.

Table 2. Response times obtained during the test campaign

	Pre vacuum non-operative test	Post vacuum non-operative test	At vacuum operative test	Post vacuum operative test
π rads / level	0.00910	0.00918	0.00918	0.00887
Rise time (ms)	3.77 ± 0.03	4.22 ± 0.05	4.0 ± 0.1	3.3 ± 0.1
Fall time (ms)	23.2 ± 0.2	26.37 ± 0.08	23.3 ± 0.1	22.5 ± 0.9
RMS	1.27	1.65	1.39	1.32

6. DISCUSSION

These preliminary results show that this particular LCOS model may be suitable for space applications. However some issues need to be revisited: the poor vacuum level obtained (1 mbar) may be actually more challenging for the electronics, however this still needs to be improved in order to obtain a proper space simulation. Surface flatness measurements may be also improved by setting a moving reference mirror. A more robust fringe analysis algorithm will provide more accurate results. In any case a full validation campaign is still pending, this includes vacuum, particle, ionizing and non-ionizing radiation tolerance and the thermal environment (typically mission dependent).

7. CONCLUSIONS

A commercial multi-purpose LCOS device has been found to perform well under vacuum conditions. No sign of degradation has been observed after non-operative and operative tests. This is relevant since no special care or modification has been performed to the device. We believe this shows that this is a promising technology. The LCOS system may be promoted to a higher TRL, and display its full potential in a space application.

REFERENCES

- [1] Haellstig, E., Stigwall, J., Lindgren, M. and Sjoqvist, L., "Laser beam steering and tracking using a liquid crystal spatial light modulator," Proceedings of SPIE, Laser System Technology 5087, (2003).
- [2] Toyoda, H., Inoue, T. and Hara, T., "Application of liquid crystal on silicon spatial light modulator (LCOS-SLM) for manipulation and sensing," IEEE, 14th Workshop on information Optics 15399552 (2015).
- [3] Graham, A., Kopp, G. A., Vargas-Aburto, C. and Uribe, R., "Preliminary space environment tests of nematic liquid crystals," Proceedings of SPIE, Photonics for space environment IV, 2811, October 1996.
- [4] Álvarez-Herrero, A., Uribe-Patarollo, N., García-Parejo, P., Vargas, J., Heredero, R. L., Restrepo, R., et al. "Imaging polarimeters based on liquid crystal variable retarder: an emergent technology for space instrumentation," Proceedings of SPIE, Polarization Science and Remote Sensing V, 8160 (2011).
- [5] Silva-López, M., Bastide, L., Restrepo, R., García Parejo, P. and Álvarez-Herrero, A., "Evaluation of a liquid crystal based polarization modulator for a space mission thermal environment," Sensors and Actuators A: Physical 266, 247-257 (2017).
- [6] Ziemkiewicz, M., Davis, S. R., Rommel, S. D., Gann, D., Luey, B., Gamble, J. D. and Anderson, M., "Laser-based satellite communication systems stabilized by non-mechanical electro-optic scanners," Proceedings of SPIE, Airborne Intelligence Surveillance, Reconnaissance Systems and Applications XIII, 982808 (2016).
- [7] European Cooperation for Space Standardization (ECSS), "Adoption Notice of ISO 16290, Space systems – Definition of the Technology Readiness Levels (TRLs) and their criteria of assessment," ECSS-E-AS-11C Requirements and Standards Division, Noordwijk, The Netherlands, (October 2014). <http://ecss.nl>
- [8] Browar, A. E. M., Shusteff, M., Pana, R. M., Ellis, J. D. and Spadaccini, C. M., "Overview and comparison of spatial light modulator calibration methods," Lawrence Livermore National Laboratory, 31st ASPE annual meeting, 686901. Portland, United States. October 2016.
- [9] Osten, W., Kohler, C. and Liesener, J., "Evaluation and application of spatial light modulators for optical metrology," *Óptica Pura y Aplicada* 38(3), 71-79 (2005).
- [10] Utsumi, Y., Kamei, T., Naito, R. and Saito, K., "Measurement Methods of Nematic Liquid Crystal Response Time," *Molecular crystals and liquid crystals* 434:1, 9/[337]-24/[352], 2017.
- [11] Wang, H. and Wu, T. X., "Correlations between liquid crystal director reorientation and optical response time of a homeotropic cell," *Journal of Applied Physics*, 95(10) 5502-5508 May 2004.
- [12] Malacara, D., [Optical Shop Testing], Wiley-Interscience Publication, Second Edition, (1992).
- [13] Itoh, K., "Analysis of the phase unwrapping problem," *Applied Optics* 21(14), July 1982.
- [14] Serati, S. and Stockley, J., "Advances in liquid crystal based devices for wavefront control and beamsteering," Proceedings of SPIE, Advanced wavefront control: methods, devices and applications III, 58940K (2005).